Aquatic Mammals 2007, *33*(1), 14-23, DOI 10.1578/AM.33.1.2007.14

Improved Techniques of Evoked-Potential Audiometry in Odontocetes

Alexander Ya. Supin and Vladimir V. Popov

Institute of Ecology and Evolution, Russian Academy of Sciences, 33 Leninsky Prospect, 119071 Moscow, Russia; E-mail: alex_supin@sevin.ru

Abstract

Efficiency of the auditory evoked-potential (AEP) method of audiometry in odontocetes can be markedly increased by the use of (1) stimulus parameters providing maximal AEP amplitude and (2) methods of better extraction of AEP from background noise. A train of short tone pips is a very effective stimulus that allows using the same analysis technique as the sinusoidally amplitude-modulated (SAM) stimulus, but provides much higher AEP amplitude. For AEP extraction from background noise, apart from a commonly used averaging method (mean-based extraction), median-based extraction is very effective when the noise is not stationary and includes short, but big spikes or bursts.

Key Words: odontocetes, hearing, audiometry, evoked potentials

Introduction

The evoked-potential method became very widely used for audiometry in odontocetes. Contrary to behavioral (psychophysical) methods, the evoked-potential investigation of hearing abilities does not require long training of the subject, is not as time-consuming, and therefore may be used in short-term captivity conditions (on the catch-and-release basis) or even in wild conditions (e.g., for investigation of stranded animals). To a large extent, the productivity of the method just for investigation of odontocetes is determined by the unique features of the odontocete auditory system. Hypertrophy of the auditory nerve centers of these animals results in very high amplitude of auditory evoked potentials (AEPs). In particular, the most widely used evoked-potential type, the non-invasively recorded auditory brainstem response (ABR), reaches a few tens of microvolts in some species, whereas in humans it regularly is below 1 μV (see review in Supin et al., 2001). The rather high evoked-response amplitude allows rather precise measurements at near-threshold stimulus intensities. In many other mammals and humans, this procedure is practically impossible because of the inability to detect response to near-threshold stimuli.

The history of the use of evoked-potential methods for audiometry in odontocetes originates from a pioneer study by Bullock et al. (1968), who invasively, in acute experiments, recorded evoked potentials from the brainstem of a few odontocete species using electrodes implanted directly to the investigated brainstem nuclei. Although it was the very first attempt of evoked response recording in cetaceans, the authors not only described main features of evoked responses, but also managed to measure some important parameters of the auditory system, including threshold measurements. Later, similar recordings through implanted electrodes were performed by Voronov & Stosman (1977).

The next step in elaborating the evoked-response diagnostic technique in odontocetes was the demonstration of the possibility for recording ABRs distantly. This method was still invasive (via intracranial electrode positions), but it did not require exact electrode implantation into the investigated brainstem nucleus (Ladygina & Supin, 1970; Bullock & Ridgway, 1972). Although these studies did not include measurements of hearing parameters, they showed that in odontocetes, the far electric field of the brainstem evoked potentials is powerful enough to be recorded at a significant distance from the field generator. Thus, these studies directed us to search for a possibility to record AEPs non-invasively—that is, from the body surface without the use of surgery.

It should be noted that since the 1970s, the non-invasive recording of ABRs has been used as a diagnostic procedure in humans (see review, Moore, 1983); however, because of the low amplitude of this response in humans (around 1 μV or less), even with the use of averaging of hundreds of individual records, satisfactory extraction of this response from background noise is possible only at high-intensity and wide-band stimuli. Therefore, in humans, ABRs are almost never used for threshold measurements, and the diagnostics

are based on the presence of all components, interwave delays, and so on.

In dolphins, ABRs were recorded truly noninvasively by Popov & Supin (1985). They showed that ABR amplitude was high enough to extract significant responses from the background noise (even at low near-threshold stimulus intensities), so ABR thresholds were measured at a number of sound frequencies (i.e., the ABR audiogram was obtained). More detailed audiometric measurements based on the ABR technique were summarized later (Popov & Supin, 1990a, 1990b).

Further elaboration of evoked-potential audiometry in odontocetes was based on the use of rhythmically modulated sound stimuli instead of single clicks or tone pips. Again, the use of such stimuli for audiometry was possible because of the unique properties of the odontocete auditory system. It has a very high temporal resolution that makes it capable of responding to sound modulation with a rate of up to 1,000 Hz or more (Dolphin, 1995; Dolphin et al., 1995; Supin & Popov, 1995a, 1995b; Popov & Supin, 1998). The evoked-potential response to such stimuli (the envelope-following response [EFR] or rate-following response [RFR]) is nothing but a high-rate rhythmic sequence of ABR. Contrary to single-stimuli, however, the multicycle response may be more confidently extracted from background noise, in particular, by the use of Fourier analysis to detect the presence of stimulation frequency in the response.

To provoke EFR in audiometric investigations of odontocetes, mostly the sinusoidally amplitude-modulated (SAM) sound stimuli are used. This kind of stimulus is a carrier tone amplitude-modulated by a function looking as $1+\sin(2\pi ft)$ or $1+\cos(2\pi ft)$, where f is the modulation rate and t is time. There are two main manners to present SAM stimuli: (1) steady-state and (2) short-burst. With the steady-state manner, a continuous SAM signal is presented throughout all the time of data collection. To extract the response from noise, fractions of the continuous record containing one or a few response cycles are averaged and the resulting averaged record is subjected to Fourier transform to evaluate the magnitude of the response at the modulation frequency (Dolphin, 1995; Dolphin et al., 1995). With the short-burst presentation manner, SAM signals are presented as bursts lasting 10 to 30 ms separated by several times longer silent intervals (Supin & Popov, 1995a, 1995b; Popov & Supin, 1998). The advantage of the last manner of presentation is that it allows observation of the response dynamic; in particular, a few millisecond lag of the response relative to the stimulus burst is an ideal control, assuring that the response is of a physiological origin, not a physical artifact.

Using either short-pip stimulation in conjunction with an ABR recording or SAM stimulation in conjunction with an EFR recording, either complete or partial audiograms of a few odontocete species were obtained: the harbor porpoise (*Phocoena phocoena*) (Popov et al., 1986), bottlenose dolphin (*Tursiops truncatus*) (Popov & Supin, 1990a), beluga whale (*Delphinapterus leucas*) (Popov & Supin, 1987; Klishin et al., 2000), common dolphin (*Delphinus delphis*) (Popov & Klishin, 1998), Amazon river dolphin (*Inia geoffrensis*) (Popov & Supin, 1990c), killer whale (*Orcinus orca*) (Szymanski et al., 1999), striped dolphin (*Stenella coeruleoalba*) (André et al., 2003), and finless porpoise (*Neophocaena phocaenoides*) (Popov et al., 2005).

All of these studies were performed using the techniques elaborated from 1985 to 1995. These techniques demonstrated very high efficiency and have not been modified, except for small details, during the last decade. The challenge to find ways to increase the efficiency of these techniques remains. This paper summarizes the results of some of these attempts.

Effective Stimuli to Produce EFR

Among its many advantages, the method of SAM stimulation features a significant disadvantage—the small amplitude of EFR produced by such stimuli at near-threshold intensities. This feature of EFR is demonstrated by a typical family of records presented in Figure 1, which presents EFR records to SAM tones of 64 kHz carrier frequency and 1 kHz modulation rate. Definite high-amplitude responses were evoked by stimuli of rather high intensities, from 150 to 120 dB re 1 μPa. At lower intensities (≤ 110 dB), EFR hardly could be visually detected (Figure 1A). Nevertheless, Fourier analysis allowed us to detect a peak at the modulation rate (1 kHz) at intensities down to 80 to 90 dB (Figure 1B). Thus, the EFR amplitude vs stimulus intensity function looked as shown in Figure 2 (1). Within a near-threshold range of 75 to 95 dB, EFR amplitude rose with intensity. Being approximated by a straight regression line (2), this part of the plot indicated a threshold of 75 dB. At higher intensities (95 to 110 dB), EFR amplitude remained very low (50 to 70 nV rms) and independent of intensity. At very high intensities (≥ 115 dB), EFR amplitude rose steeply. Detection of low-amplitude (< 50 nV rms) EFR was possible only at very good quality of records, with a background noise level of about 10 nV. If the noise level of the record were a bit higher (line 3 in Figure 2), only responses to stimulus intensities > 110 dB would be detectable, and approximation of this part of the experimental plot by a regression line (line 4 in

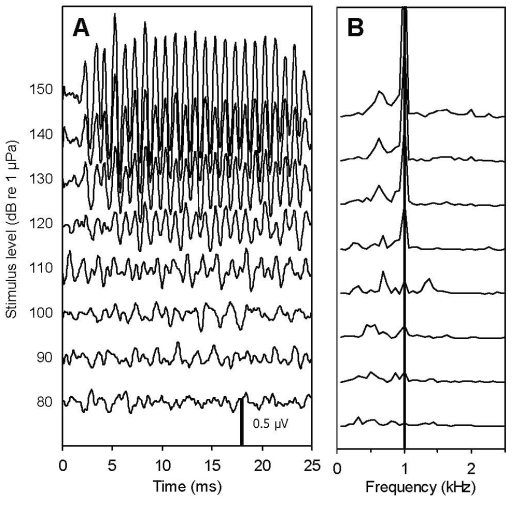

Figure 1. A. EFR records obtained from a bottlenose dolphin at various intensities of SAM stimuli, and B. their frequency spectra; SAM stimulus carrier frequency is 64 kHz, modulation rate is 1 kHz, modulation depth is 100%, burst duration is 20 ms, and intensity (dB rms re 1 µPa) is specified near the records. Vertical line in B marks spectrum peaks at the modulation frequency of 1 kHz.

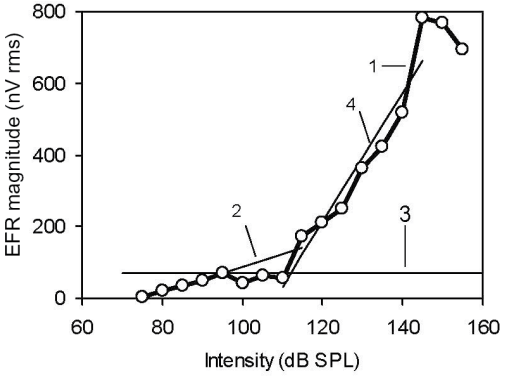

Figure 2. EFR magnitude dependence on stimulus intensity (data presented in Figure 1); 1 – experimental data, 2 – linear approximation of the near-threshold part of the experimental plot, 3 – critical level of background noise for detecting the near-threshold responses, and 4 – linear approximation of the supra-threshold part of the experimental plot.

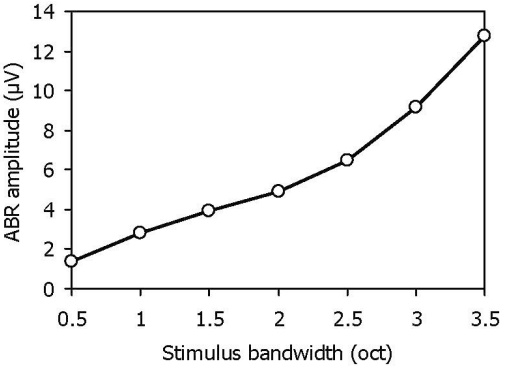

Figure 3. Dependence of maximal available ABR amplitude on stimulating tone-pip bandwidth, from 0.5 octaves (11.5 to 16 kHz) to 3.5 octaves (11.5 to 128 kHz)

Figure 2) would result in a false threshold estimate of 107 dB (i.e., with a 32-dB error). This example demonstrates that the use of SAM-EFR testing requires a very high quality of records which is not always available (e.g., when investigation is done in field conditions).

The cause of the low response amplitude to SAM stimuli is obvious. Popov & Supin (2001) showed that ABR amplitude depends to a much larger extent on the stimulus frequency bandwidth rather than on spectrum level. This regularity is demonstrated by Figure 3, which shows ABR amplitude as a function of tone-pip bandwidth, from 0.5 oct (11.2 to 16.0 kHz) to 3.5 oct (11.2 to 128.0 kHz). The maximal available ABR amplitude rose from 1.4 to 12.8 µV (i.e., more than 9 times). Indeed, the wider the stimulus frequency bandwidth, the larger the part of the Organ of Corti is stimulated and the more neuronal units in the auditory system contribute to ABR generation. EFR in odontocetes is a high-rate rhythmic sequence of ABRs, so it displays the same regularity. The bandwidth of SAM stimuli is rather narrow—it is $\pm f$, where f is the modulation rate.

To produce EFR in odontocetes, modulation rates of 0.6 to 1.0 kHz mostly are used. Thus, the bandwidth of SAM stimulus is as narrow as ± 0.6 to ± 1.0 kHz. Therefore, this stimulus produces a low-amplitude response when the stimulus is of moderate intensity (< 110 dB in Figure 2). At very high intensities (> 115 dB in Figure 2), EFR amplitude steeply increases, most likely because of the "internal spectrum splatter" wherein intensive stimuli excite wider regions of the Organ of Corti than the representation of the stimulus bandwidth.

This explanation of EFR amplitude dependence on SAM stimulus intensity gives a clue to making stimuli more effective for producing EFR. The obvious solution of the problem is to enlarge the stimulus bandwidth. The simplest way to do it is to use a signal as a rhythmic pip train, with each pip shorter then the modulation rate. Signals composed of cosine-enveloped tone pips of various durations are exemplified in Figure 4. The modulation rate of all the signals is 1 kHz, but the pip duration is different: 1 ms in Figure 4A (this is the SAM waveform), 0.5 ms in Figure 4B, and 0.25 ms in Figure 4C. Respectively, the frequency spectrum (Figure 4E) of the signal in Figure 4B is twice as wide as the spectrum (Figure 4D) of the

SAM signal (Figure 4A), and the spectrum (Figure 4F) of the signal in Figure 4C is four times wider.

Our investigation showed that shortening the pip duration markedly enhances the EFR. In Figure 5, EFR records are obtained using pip-train stimulus with the pip rate of 1 kHz, but the pip duration of 0.25 ms. A comparison with Figure 1 (EFR to SAM stimuli) shows much higher response amplitude in the near-threshold intensity range, which makes the response detection much more confident.

In more detail, the data on EFR dependence on the tone-pip duration are summarized in Figure 6. It presents EFR magnitude as a function of stimulus intensity, taking the pip duration as a parameter. The pip rate of 1 kHz was equal for all the plots, but the pip duration varied by two-fold steps from 1 ms (SAM signal) to 0.062 ms. Respectively, the stimulus frequency bandwidth varied from 1 to 16 kHz. The plots demonstrate clearly that the shorter the pips (the wider the stimulus spectrum), the higher the response amplitude and the steeper the amplitude dependence on intensity in the near-threshold range. It is obvious that the steepest plots (at 0.062 to 0.125-ms pip duration) allow a threshold to be detected much more precisely than the shallowest one (at 0.500 to 1-ms pip duration).

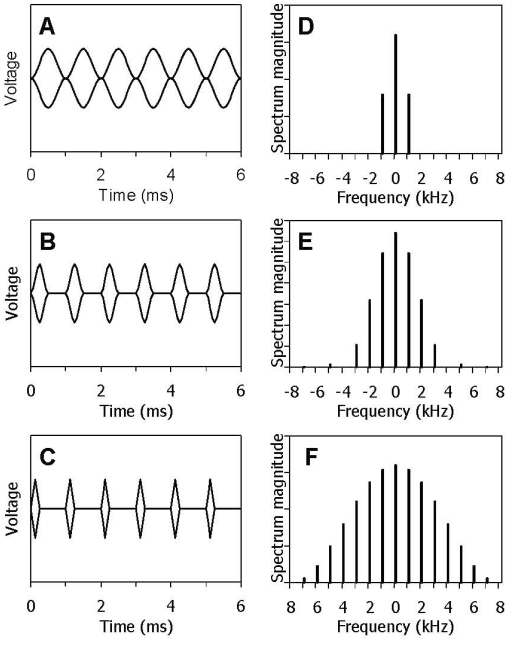

Figure 4. Envelopes of pip-train signals of 1 kHz pip rate and different pip durations: A. 1 ms, B. 0.5 ms, and C. 0.25 ms, and their frequency spectra (D to F, respectively); in D through F, frequency is specified in kHz relative to the carrier frequency.

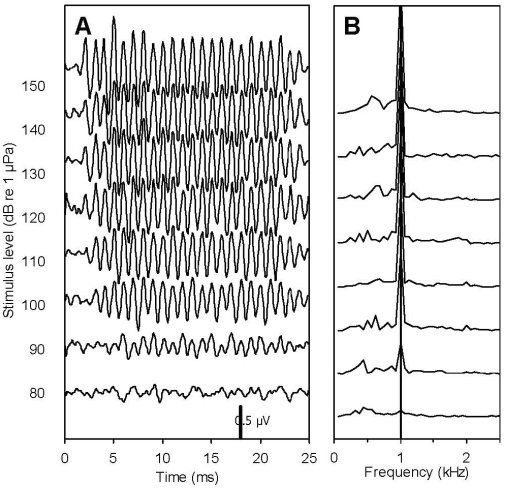

Figure 5. A. EFR records obtained at various intensities of pip-train stimuli, and B. their frequency spectra; stimulation and recording conditions and designations are the same as in Figure 1, except stimulation pip duration is 0.25 ms rather than 1 ms.

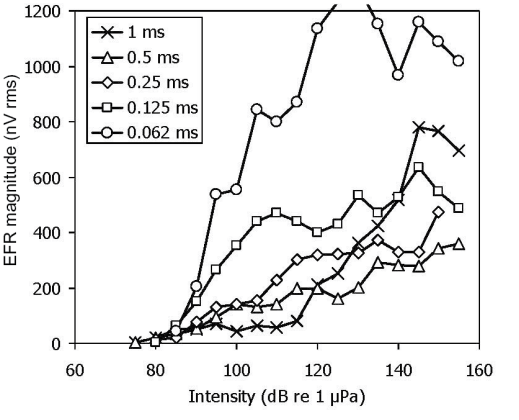

Figure 6. EFR amplitude dependence on pip-train stimulus intensity, taking the pip duration (0.062 to 1 ms) as a parameter; stimulus carrier frequency is 64 kHz, pip rate is 1 kHz, and stimulus intensity is specified in dB re 1 µPa rms of the pip (not including inter-pip pauses).

Of course, the pip duration cannot be shortened infinitely when used for audiometry. The shorter the pip and wider the spectrum, the more ambiguously the found threshold can be attributed to a certain carrier frequency. Thus, the minimal pip duration is dictated by the required precision of the audiogram on the frequency scale. For the majority of cases, an audiogram obtained with a ¼- to ½-oct step may be considered as detailed enough. For such cases, a pip may contain not more than 8 to 10 carrier cycles. For example, a 8-cycle pip at a carrier frequency of 128 kHz has a

spectrum bandwidth (at the half-level) of ± 128/8 = ± 16 kHz, which corresponds to 0.36 oct.

When using short-pip trains for audiometry, which measure of the stimulus intensity (peak, peak-equivalent, rms, or other) is appropriate to characterize the threshold? Indeed, pip trains of one and the same pip rate and pip peak level, but of different pip durations, have different rms levels (if rms is computed by integration throughout all of the train). This difference is illustrated by Figure 7, which exemplifies two pip trains of 1 kHz pip rate composed of 1-ms (Figure 7A) and 0.25-ms long pips (Figure 7B). Both trains are of one and the same peak levels; respectively, their peak-equivalent levels are equal, and their rms levels are equal, too, if calculated within the duration of the pip. If the rms level is computed throughout the train (i.e., including both the pips and inter-pip silent interval), the level of the train (B) is four times less (–6 dB) than that of the train (A). Which intensity measure should be taken to characterize a threshold—the level of each pip or the overall level of the train? The answer depends on the integration time within the auditory system. If it is markedly shorter than the inter-pip interval (i.e., each pip acts as an independent stimulus), the intensity of a separate pip should be taken as the stimulus level; if the integration time is comparable or longer than the inter-pip interval, the overall train level should be taken.

There were several estimates of the integration time in the auditory system of odontocetes. Both behavioral (Vel'min & Dubrovskiy, 1975; Moore et al., 1984; Au et al., 1988; Au, 1990; Dubrovskiy, 1990) and evoked-potential (Supin & Popov, 1995b, 1995c; Popov & Supin, 1997) experiments showed the limit of temporal resolution in the odontocete auditory system as short as 0.25 to 0.35 ms. On the other hand, Popov & Supin (1990a) and Supin & Popov (1995b) showed that in a near-threshold intensity range, the integration time of evoked potentials may be prolonged up to a few microseconds. In behavioral experiments in dolphins, integration times were tens or hundreds of milliseconds (Johnson, 1968). Thus, depending on the conditions and applied test, oftentimes the integration time of the odontocete auditory system may vary. Therefore, direct measurements were necessary to find out how the integration time influences the threshold estimates obtained with different test-pip durations.

Results of such measurements are presented in Figure 8, which shows threshold measurements with the use of test trains of 1 kHz pip rate in one and the same subject, at one and the same carrier frequencies, but with different test-pip durations. The results are presented in two manners: (1) as short-term rms levels (i.e., by computing rms over the duration of the pip only, not including the inter-pip silent pause) and (2) as long-term rms (i.e., by computing rms throughout the overall pip train, including both the pips and pauses). Threshold estimates presented in short-term rms are dependent on pip duration: to reach the threshold, shorter pips require higher amplitude than longer pips. The rate of this dependence is around 3 dB when the pip duration is doubled, so, being presented as long-term rms, the same data feature

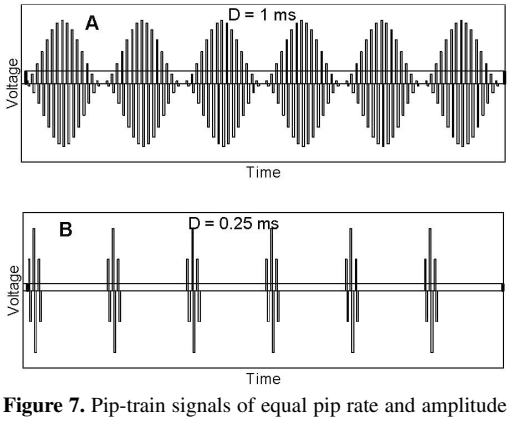

Figure 7. Pip-train signals of equal pip rate and amplitude but of different pip durations—in A. these are four times longer than in B. horizontal lines show rms levels computed throughout the signal duration, including both the pips and inter-pip pauses.

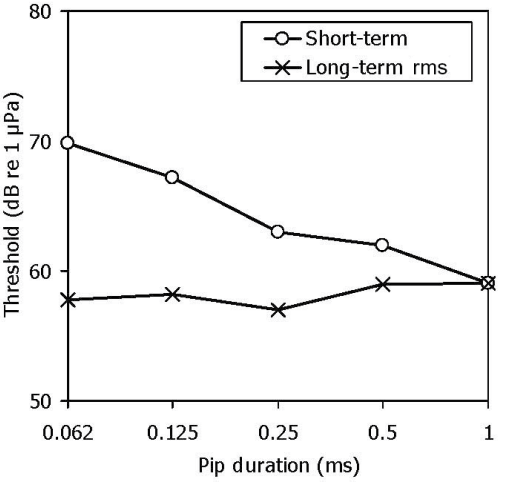

Figure 8. EFR-estimated thresholds obtained at a carrier frequency of 64 kHz, at a pip rate of 1 kHz, and at different pip durations from 0.062 to 1 ms; one and the same set of data is presented in two manners: as short-term rms (computed over pip duration, not including inter-pip pauses) and as long-term rms (computed throughout the stimulus duration, including both the pips and inter-pip pauses).

negligible dependence of the threshold on pip duration. This result indicates that the temporal integration time of the odontocete auditory system is long enough to summarize the stimulus energy at least up to 1 ms and, therefore, the long-term rms is a more adequate measure of the stimulus level in threshold measurements with the use of pip-train stimuli.

The adequacy of the long-term rms measure to specify stimulus intensity in pip-train threshold measurements is further confirmed by comparing complete audiograms obtained with the use of different stimuli. Figure 9 presents two audiograms obtained in one and the same subject in similar conditions, but with different test stimuli. Audiogram 1 was obtained with the use of test stimulus of a pip rate of 1 kHz and pip duration of 1 ms (i.e., the SAM stimulus); its intensity was specified as rms value (short- and long-term rms measures coincide for SAM signals). Audiogram 2 was obtained with the use of stimulus of the same pip rate and with a pip duration of 0.25 ms; its intensity was specified as long-term rms. The audiograms almost coincided, except Audiogram 2 was less scattered, which was a result of a more confident threshold detection.

Thus, the use of short-pip trains, instead of true SAM test stimuli, makes the audiometric measurements more precise and confident.

Methods of Extraction of Evoked-Potential Signals from Noise

Although AEP amplitude in odontocetes is, keeping other conditions equal, much higher than in the majority of other mammals, it does not exceed a few microvolts or tens of microvolts in the best cases and is as low as tens or hundreds of nanovolts

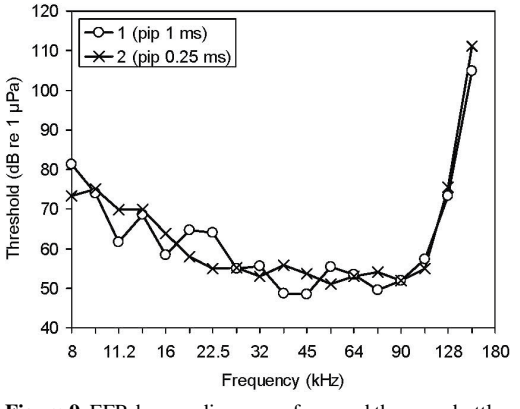

Figure 9. EFR-base audiograms of one and the same bottlenose dolphin obtained with the use of different pip durations: 1 and 0.25 ms, as indicated; thresholds are specified as long-term rms of the threshold stimulus.

at near-threshold intensities. These levels are well below the level of electrical background noise. Even if the input noise of the evoked-potential amplifier is very low (which is readily available with the use of modern electronic components), noise of biogenic origin (myogenic, cardiogenic, and others) within a frequency band of a few kHz (which is necessary to record ABR) may be as high as a few tens of microvolts. Therefore, computational methods of extraction signals from noise are always used for non-invasive evoked-potential audiometry in odontocetes.

A commonly used method of signal extraction from background noise is the coherent averaging procedure. For that, a few hundred to a thousand individual records synchronized by the stimulus are averaged. If the noise is statistically constant, summarizing individual records results in summarizing the noise energy (i.e., its amplitude increases proportionally to $N^{0.5}$).

where, N is the number of summarized individual records,

whereas a coherent signal summarizes proportionally to N; the result is improvement of the signal-to-noise ratio as $N^{0.5}$. For example, the averaging of 1,000 individual records improves the signal-to-noise ratio by 31.6 times.

In real experimental conditions, however, the background noise may be nonconstant. A few big spikes or high-level noise bursts may spoil the final averaged records if their amplitude remains high enough even after division by the averaging number. The influence of big noise spikes or bursts on the results of the averaging procedure is modeled in Figure 10. Figure 10A presents a signal, and Figure 10B presents 10 records of the same signal in statistically constant noise (thin lines). The standard averaging procedure satisfactorily extracts the original signal from such noise. The averaged record (solid line) is very similar to the original. If only one of the original records contains a big noise burst, however, it desperately spoils the final result; the averaged record has little in common with the original (Figure 10C).

A commonly adopted way to avoid this effect is to reject the individual records containing high-amplitude signals. This method, although effective enough, has some disadvantages. It implies an arbitrary and voluntary criterion of the maximal allowed amplitude of the signal and markedly slows down the data acquisition because all the high-signal records are rejected, whereas only small parts of them may be significantly contaminated by an artifact.

We supposed that there was a more logical method to diminish the influence of high-amplitude artifacts on the signal extraction procedure. Indeed, the standard averaging procedure is finding

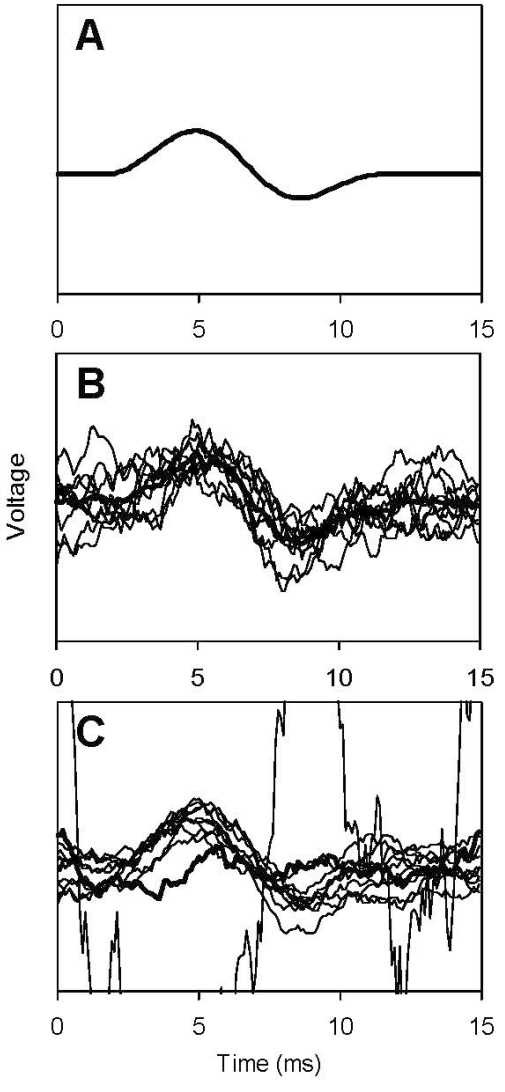

Figure 10. Modeling of average-based extraction of a signal from noise at different noise features; A. original signal, B. 10 samples of the signal contaminated by statistically stationary noise (thin lines) and their average (solid line), and C. the same when one of the samples contains a high-amplitude noise wave.

the mean of distribution of voltages across a scan (we use the term "scan" for the array of data in all the averaged records at a certain instant). The mean is not the only parameter to characterize the position of the distribution at the voltage axis. Two others are the mode and the median. In a normal distribution, values of all these three parameters coincide, so any of them can be taken to characterize the position of the distribution, and the mean is the easiest to compute. In a non-normal distribution, these parameters may be significantly different, thus, a reasonable question is "Which of them is the best to characterize the position of the distribution at the voltage axis?"

Contrary to the mean, the mode and median are not sensitive to a large deviation of a small part of the distribution from its main part. This is illustrated by a simple example in Figure 11. Figure 11A presents a normal distribution in which the mean, mode, and median coincide. Distribution in Figure 11B differs from that in Figure 11A only by moving a small part of it to higher values (i.e., in a small number of cases, the value of the distributed variable greatly increased). The mean of the modified distribution markedly shifted to higher values; however, the mode did not shift because the most probable value of the variable remained the same. The median also did not shift because the shift of the upper part of the distribution did not change the number of cases below and above the initial median value.

Practical computation of the mode is very error-sensitive because it is based on counting a small number of values within a small voltage interval. The median can be easily computed, however, and

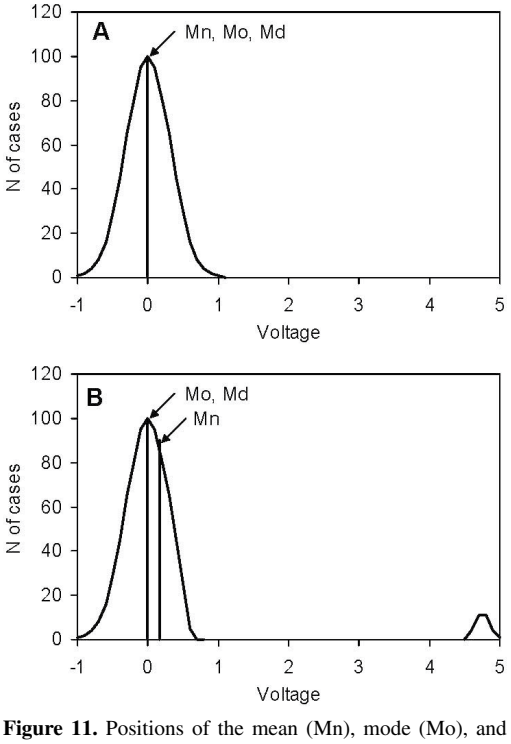

Figure 11. Positions of the mean (Mn), mode (Mo), and median (Md) at different forms of distribution; A. normal distribution (the mean, mode, and median coincide), and B. deformed distribution (the mode and median remain at the same position; the mean is shifted to the right).

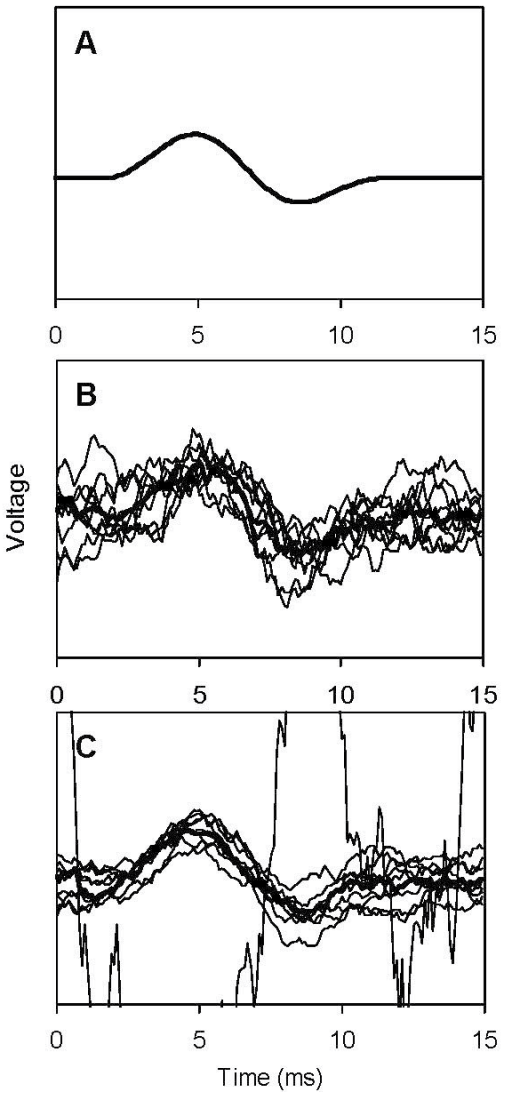

Figure 12. Modeling of median-based extraction of a signal from noise at different noise features; the same set of samples and the same designations as in Figure 10, except medians instead of means are presented by solid lines.

provides a convenient estimate of the value of the extracted signal, independent of high-amplitude noise spikes. It is illustrated by Figure 12, which presents an analysis of the very same array of noise-contaminated signals as in Figure 10. Again, Figure 12A presents the original signal waveform. When the noise is uniform (Figure 12B), the median-based extraction of the signal gives a good result, almost the same as the mean-based extraction. When the noise contains a big spike (Figure 12C), the result of extraction remains almost the same (i.e., much better than with the use of the mean-based extraction) (compare to Figure 10C).

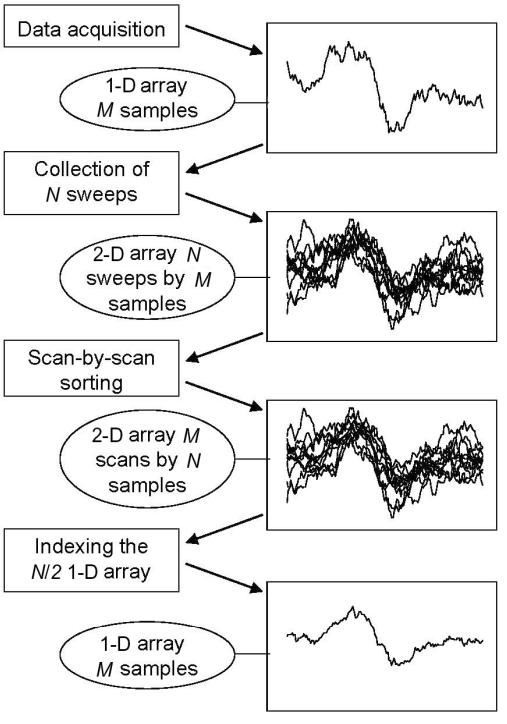

Figure 13. Successive steps of online median-based extraction of signals from noise; operations are listed in rectangles and the results in ovals.

Thus, the median-based extraction of AEPs from noise may be very effective in cases of non-uniform noise containing a small number of high-amplitude artifacts. In such cases, the method provides a more reliable extraction of AEPs and a more precise audiometric measurement than the classic mean-based extraction.

Median-based extraction of AEPs may be realized by a variety of algorithms. Figure 13 presents main blocks of a program for online median-based AEP extraction realized using *LabView*® (National Instrument) technology. Each data acquisition cycle results in the collection of a sweep—a 1-D array of *M* samples. Repetition of *N* cycles results in the collection of a 2-D array composed of *N* sweeps by *M* samples or, all the same, *M* scans by *N* samples. Each scan of this array is sorted so that all samples in a scan are arranged orderly by their values, from minimal to maximal. The mean sample of an index of *N/2* in each of the sorted scans belongs to the median. Thus, the 1-D array of an index of *N/2* is the searched-for AEP waveform extracted by the median-based procedure.

Conclusions

The evoked-potential method, although widely used for a long time for audiometry in odontocetes, may need further elaboration and improvement. The modifications of the method described herein make it possible to perform audiometric measurements more easily and precisely, thus enlarging the usage area of the evoked-potential audiometry.

Acknowledgments

The study was supported by The Russian Ministry of Science and Education, Grant NSh-7117.2006.4. A travel grant provided to A. Ya. Supin by the U.S. Office of Naval Research to attend the ECS meeting where this paper was presented is greatly appreciated.

Literature Cited

André, M., Supin, A., Delory, E., Kamminga, C., Degollada, E., & Alonso, J. M. (2003). Evidence of deafness in a striped dolphin, *Stenella coeruleoalba*. *Aquatic Mammals*, *29*(1), 3-8.

Au, W. W. L. (1990). Target detection in noise by echolocating dolphins. In J. A. Thomas & R. A. Kastelein (Eds.), *Sensory abilities of cetaceans: Laboratory and field evidence* (pp. 203-216). New York: Plenum.

Au, W. W. L., Moore, P. W. B., & Pawloski, D. A. (1988). Detection of complex echoes in noise by an echolocating dolphin. *Journal of the Acoustical Society of America*, *83*, 662-668.

Bullock, T. H., & Ridgway, S. H. (1972). Evoked potentials in the central auditory system of alert porpoises to their own and artificial sounds. *Journal of Neurobiology*, *3*, 79-99.

Bullock, T. H., Grinnell, A. D., Ikezono, F., Kameda, K., Katsuki, Y., Nomoto, M., et al. (1968). Electrophysiological studies of the central auditory mechanisms in cetaceans. *Zeitschrift für Vergleichende Physiologie*, *59*, 117-156.

Dolphin, W. F. (1995). Steady-state auditory-evoked potentials in three cetacean species elicited using amplitude-modulated stimuli. In R. A. Kastelein, J. A. Thomas, & P. E. Nachtigall (Eds.), *Sensory systems of aquatic mammals* (pp. 25-47). Woerden, The Netherlands: De Spil.

Dolphin, W. F., Au, W. W. L., & Nachtigall, P. E. (1995). Modulation transfer function to low-frequency carriers in three species of cetaceans. *Journal of Comparative Physiology A*, *177*, 235-245.

Dubrovskiy, N. A. (1990). On the two auditory systems in dolphins. In J. A. Thomas & R. A. Kastelein (Eds.), *Sensory abilities of cetaceans: Laboratory and field evidence* (pp. 233-254). New York: Plenum.

Johnson, C. S. (1968). Relation between absolute threshold and duration of tone pulse in the bottlenosed porpoise. *Journal of the Acoustical Society of America*, *43*, 757-763.

Klishin, V. O., Popov V. V., & Supin, A. Ya. (2000). Hearing capabilities of a beluga whale, *Delphinapterus leucas*. *Aquatic Mammals*, *26*, 212-228.

Ladygina, T. F., & Supin, A. Ya. (1970). Acoustic projection in the dolphin's cerebral cortex. *Fisiologicheskiy Zhurnal SSSR* (*Physiological Journal of USSR*), *56*, 1554-1560.

Moore, E. J. (Ed.). (1983). *Bases of auditory brain stem evoked responses*. New York: Grune and Stratton. 481 pp.

Moore, P. W. B., Hall, R. W., Friedl, W. A., & Nachtigall, P. E. (1984). The critical interval in dolphin echolocation: What is it? *Journal of the Acoustical Society of America*, *76*, 314-317.

Popov, V. V., & Klishin, V. O. (1998). EEG study of hearing in the common dolphin, *Delphinus delphis*. *Aquatic Mammals*, *24*(1), 13-20.

Popov, V. V., & Supin, A. Ya. (1985). Determining the hearing characteristics of dolphins according to brainstem evoked potentials. *Doklady Biological Sciences*, *283*, 524-527.

Popov, V. V., & Supin, A. Ya. (1987). Characteristics of hearing in the beluga, *Delphinapterus leucas*. *Doklady Biological Sciences*, *294*, 370-372.

Popov, V. V., & Supin, A. Ya. (1990a). Auditory brain stem responses in characterization of dolphin hearing. *Journal of Comparative Physiology A*, *166*, 385-393.

Popov, V. V., & Supin, A. Ya. (1990b). Electrophysiological studies of hearing in some cetaceans and manatee. In J. A. Thomas & R. A. Kastelein (Eds.), *Sensory abilities of cetaceans: Laboratory and field evidence* (pp. 405-415). New York: Plenum.

Popov, V. V., & Supin, A. Ya. (1990c). Electrophysiological investigation of hearing of the fresh-water dolphin *Inia geoffrensis*. *Doklady Biological Sciences*, *313*, 488-491.

Popov, V. V., & Supin, A. Ya. (1997). Detection of temporal gaps in noise in dolphins: Evoked-potential study. *Journal of the Acoustical Society of America*, *102*, 1169-1176.

Popov, V. V., & Supin, A. Ya. (1998). Auditory evoked responses to rhythmic sound pulses in dolphins. *Journal of Comparative Physiology A*, *183*, 519-524.

Popov, V. V., & Supin A. Ya. (2001). Contribution of various frequency bands to ABR in dolphins. *Hearing Research*, *151*, 250-260.

Popov, V. V., Ladygina, T. F., & Supin, A. Ya. (1986). Evoked potentials in the auditory cortex of the porpoise, *Phocoena phocoena*. *Journal of Comparative Physiology A*, *158*, 705-711.

Popov, V. V., Supin, A. Ya., Wang, D., Wang, K., Xiao, J., & Li, S. (2005). Evoked-potential audiogram of the Yangtze finless porpoise *Neophocaena phocaenoides asiaeorientalis* (L). *Journal of the Acoustical Society of America*, *117*, 2728-2731.

Supin, A. Ya., & Popov, V. V. (1995a). Envelope-following response and modulation transfer function in the dolphin's auditory system. *Hearing Research*, *92*, 38-46.

Supin, A. Ya., & Popov, V. V. (1995b). Frequency tuning and temporal resolution in dolphins. In R. A. Kastelein,

J. A. Thomas, & P. E. Nachtigall (Eds.), *Sensory systems of aquatic mammals* (pp. 95-110). Woerden, The Netherlands: De Spil.

Supin, A. Ya, & Popov, V. V. (1995c). Temporal resolution in the dolphin's auditory system revealed by double-click evoked potential study. *Journal of the Acoustical Society of America*, *97*, 2586-2593.

Supin, A.Ya., Popov, V. V., & Mass A. M. (2001). *The sensory physiology of aquatic mammals*. Boston: Kluwer Academic Publishers. 332 pp.

Szymanski, M. D., Bain, D. E., Kiehl, K., Pennington, S., Wong, S., & Henry, K. R. (1999). Killer whale (*Orcinus orca*) hearing: Auditory brainstem response and behavioral audiograms. *Journal of the Acoustical Society of America*, *106*, 1134-1141.

Vel'min, V. A., & Dubrovskiy, N. A. (1975). Auditory analysis of sounds pulsed in dolphins. *Doklady Biological Sciences*, *225*, 562-565.

Voronov, V. A., & Stosman, I. M. (1977). Frequency threshold characteristics of subcortical elements of the auditory analyzer of *Phocoena phocoena*. *Zhurnal Evolutsionnoy Biokhimii I Physiologii* (*Journal of Evolutionary Biochemistry and Physiology*), *13*, 619-622.